COVER SHEET

Adam, Clayton J and Loughran, Jeffrey G (2004) Multi-variate analysis of frictional interaction between grooved rollers and prepared sugarcane. *Transactions of the American Society of Agricultural Engineers* 47(5):pp. 1611-1618

MULTI−VARIATE ANALYSIS OF FRICTIONAL INTERACTION BETWEEN GROOVED ROLLERS AND PREPARED SUGARCANE

C. J. Adam, J. G. Loughran

ABSTRACT. *The Australian sugar industry utilizes rolling almost exclusively for extraction of sucrose from prepared sugarcane. The feeding and extraction performance of rolling mills is strongly dependent on the friction coefficient between counter−rotating rolls and the fibro−porous sugarcane blanket. Rolls are circumferentially grooved and roughened with weld droplets to assist juice drainage and maximize friction between rolls and blanket. Previous investigators have performed experimental measurements of the friction coefficient between metal surfaces and prepared cane or bagasse. This article develops a multi−variate empirical regression equation based on the experimental measurements of previous investigators to describe the dependence of the interfacial friction coefficient on normal pressure, groove angle, and relative rubbing speed. The friction coefficient was found to decrease exponentially with increasing normal pressure, decrease linearly with increasing rubbing speed, and increase with decreasing groove angle in accordance with simple wedge theory.*

Keywords. *Friction Coefficient, Mill Feeding, Roller Grooving, Sugarcane Crushing.*

Sugarcane is a grass of the genus *Saccharum* that accounts for 70% of world sugar production. The Australian sugar industry crushes over 30 million tonnes of sugarcane per annum, producing more than four million tonnes of raw sugar. In Australia, sucrose−rich juice is extracted from the sugarcane by crushing the cane in rolling mills.

A key consideration in the design of sugarcane crushing mills is the ability of the mill to feed the shredded cane blanket at high crushing rates. The feeding performance of the mill directly affects factory throughput and sugar extraction (Crawford, 1955). The feeding ability of a particular mill is strongly dependent on the friction coefficient between the rollers and the sugarcane blanket, and recent increases in crushing rate through existing equipment have further emphasized the need for good frictional grip between rollers and the sugarcane blanket. High values of the friction coefficient are desirable for mill feeding, where the contact angles of the material on rollers are highest. Conversely, low friction is desirable in the case of sliding contact with chutes and plates.

The universally accepted industry practice of circumferentially grooving mill rollers is shown schematically in figure 1 and achieves three purposes:

- Providing increased grip on the sugarcane blanket.
- Providing flow paths for drainage of expressed juice.
- Rupturing remaining closed juice cells (increased fineness of preparation).

The increase in frictional grip obtained by using grooved rollers has been demonstrated by various researchers (Bullock, 1957; Cullen, 1965). Current industry practice suggests that roller grooving alone may not be sufficient to provide the required grip, and roll "arcing" (application of weld droplets to the tips of the grooves) is also used to improve mill feeding. The effects of roll grooving on the friction coefficient have been experimentally measured, although the increase in friction coefficient due to roll arcing remains a qualitative observation.

In Australia, significant advances in the theory and practice of sugarcane crushing were made during the period 1955−1970 with numerous experimental investigations, including measurements of the friction coefficient between prepared (shredded) sugarcane and metal surfaces. More recently, the advent of advanced computational simulation tools has led to interest in simulating the crushing process for optimization of mill feeding and extraction performance (Adam and Loughran, 2001).

This study develops multi−variate regression analyses to quantify the frictional interaction between prepared sugarcane and metal surfaces for a range of conditions, based on the direct experimental measurements of previous researchers. The regression equations represent a new tool for quantitative description of frictional interactions in numerical models of the sugarcane crushing process.

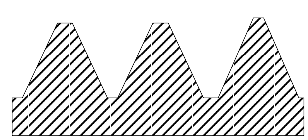

Figure 1. Sectional view of circumferential roller grooving.

Article was submitted for review in August 2003; approved for publication by the Food & Process Engineering Institute Division of ASAE in August 2004.

The authors are **Clayton James Adam,** Senior Postdoctoral Fellow, School of Mechanical, Manufacturing, and Medical Engineering, Queensland University of Technology, Brisbane, Australia; and **Jeffrey Graham Loughran,** Professor, School of Engineering, James Cook University, Townsville, Australia. **Corresponding author:** Dr. Clayton Adam, School of Mechanical, Manufacturing, and Medical Engineering, Queensland University of Technology, 2 George St, GPO Box 2434, Brisbane, QLD, Australia; phone: +61−7−3864−1377; fax: +61−7−3864−1469; e−mail: c.adam@qut.edu.au.

  ISSN 0001−2351

Direct Measurements of the Friction Coefficient

Crawford (1955), Bullock (1957), Braddock (1963), Murry (1960), and Cullen (1965) each performed direct experimental measurements of the friction coefficient between prepared sugarcane or bagasse (defined as sugarcane that has previously undergone compression) and metal surfaces. Bullock suggests that there are five main factors affecting the coefficient of friction:

- Normal pressure
- Preparation level (fineness of the shredded cane)
- Rubbing speed
- Surface condition
- Dryness of fiber.

With reference to dryness of the fiber (point 5), Murry found that the friction coefficient was not affected by moisture content, provided that a certain level of moisture was present in the material. Bullock found that the friction coefficient increased with increasing preparation (point 2), except for the case of dynamic friction on fresh prepared cane, where no significant preparation effect was observed.

This study is concerned with crushing of fresh prepared sugarcane. Accordingly, the potential effects of preparation, dryness of fiber, temperature, and maceration may all be neglected. This leaves normal pressure, rubbing speed, and surface condition as the three primary factors affecting frictional behavior. Three of the previously mentioned authors measured the effects of these variables on the friction coefficient (Bullock, 1957; Murry, 1960; and Cullen, 1965).

Bullock's extensive experimental program included both low− and high−pressure experiments over the range of conditions shown in table 1. Low−pressure experiments were performed using an experimental two−roll mill, shown schematically in figure 2. High−pressure experiments were performed in a 50 mm diameter cylindrical cell, shown schematically in figure 3. Bullock made the distinction between limiting friction, which occurs statically just before the occurrence of slip, and dynamic friction, which is the (always lower) coefficient measured during slip.

Murry's experiments were all performed at low pressure, using a variety of flat surfaces with different materials and

Table 1. Conditions for direct friction measurements (Bullock, 1957; experiments 6.2(a), 6.3, 6.4, and 6.5).

Apparatus	Friction box on two−roll mill (low pressure), Cylindrical cell (high pressure).
Cane varieties	Q50
Cane condition	Fresh prepared cane, Old prepared cane (2 weeks), Pre−crushed and boiled bagasse, Pressed and dried bagasse, Bone−dry fiber.
Preparation levels	"Coarse," "fine," "very fine," and "fibrated."
Normal pressures	0 to 620 kPa (low−pressure apparatus), 3.5 to 76 MPa (high−pressure apparatus)
Surface conditions	Low pressure: Cold−rolled smooth steel; 34°, 8.5 mm pitch grooved cast iron, med. finish. High pressure: "As cast" smooth cast iron; 45°, 8.5 mm pitch grooved cast iron, med. finish.
Rubbing speeds	Limiting or zero−speed (low and high pressure), Dynamic at 51 to 381 mm s^{-1} (low pressure).

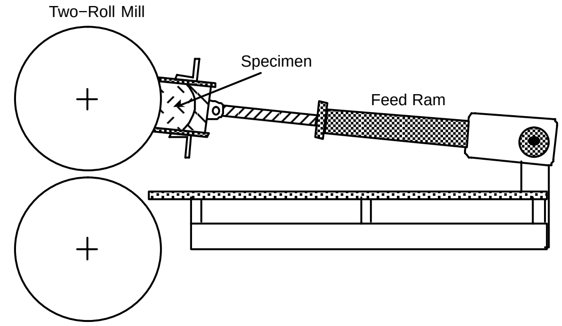

Figure 2. Low−pressure friction apparatus (Bullock, 1957).

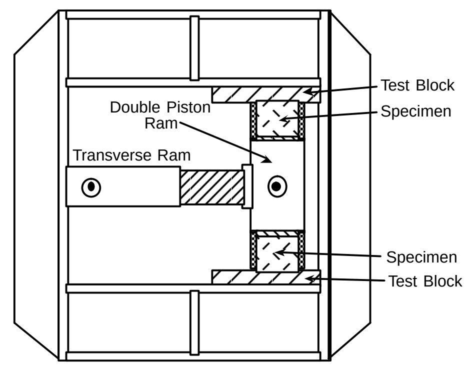

Figure 3. High−pressure friction apparatus (Bullock, 1957).

Table 2. Conditions for direct friction measurements (Murry, 1960; section 9.6).

Apparatus	Rectangular sliding block with weight (low pressure).
Cane varieties	NCo310, pindar
Cane condition	Fresh prepared cane, Rewetted kalamia bagasse.
Preparation levels[a]	500/20, 750/15, and 750/30
Normal pressures	136 kPa
Surface conditions	Machined cast iron, cast steel, and aluminum, "As cast" cast iron, cast steel, and aluminum, "Roughened surface," Just−machined cast iron (6.8−368 µm CLA), Rusted cast iron (6.8−368 µm CLA).
Rubbing speeds	Limiting or zero−speed, Dynamic at 152 mm $s^{-1.}$

[a] Preparation levels such as 750/15 refer to sugarcane shredded in a batch shredder, in this example at 750 rpm for 15 s.

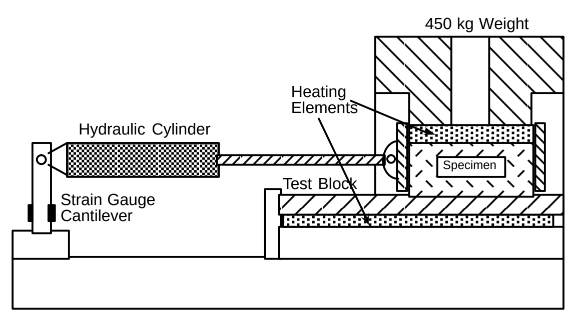

Figure 4. Low−pressure friction apparatus (Murry, 1960).

Table 3. Conditions for direct friction measurements (Cullen, 1965; chapter 6).

Apparatus	Rectangular sliding block with ram (high pressure).
Cane varieties	Unknown
Cane condition	Fresh prepared cane
Preparation levels	500/20 and 750/15
Normal pressures	2.8 to 19.3 MPa
Surface conditions	Cast iron (1.27 µm CLA), 45°, 8.5 mm pitch grooved cast iron (1.27 µm CLA), 55°,16.9 mm pitch grooved cast iron (1.27 µm CLA).
Rubbing speeds	Limiting or zero−speed, Dynamic at 9 and 42 mm s^{-1}.

surface finishes. The experimental conditions and apparatus used are given in table 2 and figure 4, respectively.

Cullen's investigation of friction at high pressures recorded both limiting and dynamic coefficients. Experimental conditions and apparatus are given in table 3 and figure 5, respectively.

Figure 6 shows a summary of friction coefficients measured by the three authors for flat iron and steel surfaces at various normal pressures. For the purposes of this figure, only limiting friction coefficients on flat surfaces are considered. Note that the data at low normal pressures appear to lie on the vertical axis only because of the scaling to show the high normal pressures reached in Bullock's tests.

Figure 6 shows a decreasing trend of friction with increasing normal pressure. However, another observation of interest is the generally higher friction values for "as cast" surfaces as opposed to machined surfaces. This is a result of the greater inherent micro−roughness for "as cast" surfaces. Murry's experiments suggested that the macro−roughness generated during machining has little effect on the friction coefficient, as does the type of material (iron or steel).

Murry also found that allowing a surface to rust significantly increases the friction coefficient. Rusting appears to increase the friction coefficient due to increased micro−roughness in the same manner as the "as cast" results discussed previously.

In addition to the decrease in friction with increasing normal pressure, all researchers found that increased rubbing speeds also decrease friction, but apparently to a lesser extent than the friction−normal pressure interaction. Further, grooved surfaces exhibit higher friction coefficients than smooth surfaces, although the influence is less at higher normal pressures. No significant effect of fineness of preparation on the friction coefficient was observed for freshly shredded sugarcane.

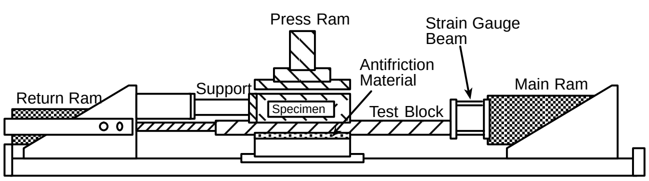

Figure 5. High−pressure friction apparatus (Cullen, 1965).

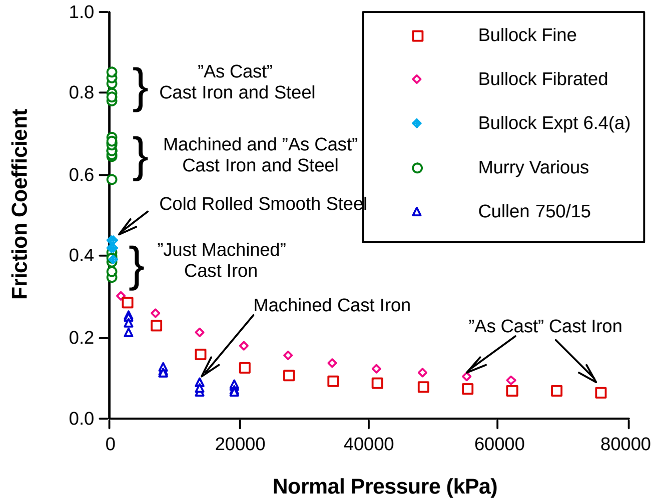

Figure 6. Limiting friction coefficients for flat surfaces.

Development of a Multi−Variate Frictional Relation

Since fineness of preparation does not significantly affect the friction coefficient, results for Bullock's "finely prepared," "very finely prepared," and "fibrated" cane are grouped together with Murry's 750/15 and 750/30 preparations and Cullen's 750/15 preparation. The limiting (static) friction coefficient is considered equivalent to a "zero−speed" value, such as occurs when the relative sliding velocity between cane and surface is zero. In this sense, both the limiting and dynamic friction measurements are subsets of an overall friction−speed relation. The remaining three experimental variables are then equivalent to the primary factors identified previously, namely normal pressure, rubbing speed, and surface condition.

The rollers of an operating mill will most likely exhibit the micro−finish of a non−rusted, machined surface, as opposed to an "as cast" or rusted surface. (Note that the overall frictional behavior will also be affected by roll arcing and grooving). For this reason, "as cast" and rusted results are omitted from further analysis. This leaves Murry's "just machined" data at low pressures and Cullen's machined cast iron data at high pressures as most representative of the conditions experienced during milling. Further, Bullock's cold−rolled smooth steel data lies close to the abovementioned low−pressure data, suggesting that its micro−finish and therefore frictional behavior is similar. We chose these three sets of experimental data for further development of the multi−variate frictional regression.

Before the regression analysis, we consider the general form of the first−order interactions of the variables, namely, "friction−normal pressure," "friction−rubbing speed," and "friction−surface condition." The "friction−surface condition" interaction has been effectively reduced to a "friction−surface geometry" interaction by selection of data for non−rusted, machined surfaces only. In terms of geometry, we assume that grooving effects can be quantified entirely in terms of the included angle of the grooves. Further, a flat surface is assumed equivalent to a grooved surface of 180° included angle. This assumption is adopted in preference to the other possible situation, where a flat surface is assumed equivalent to a grooved surface of 0° included angle. The

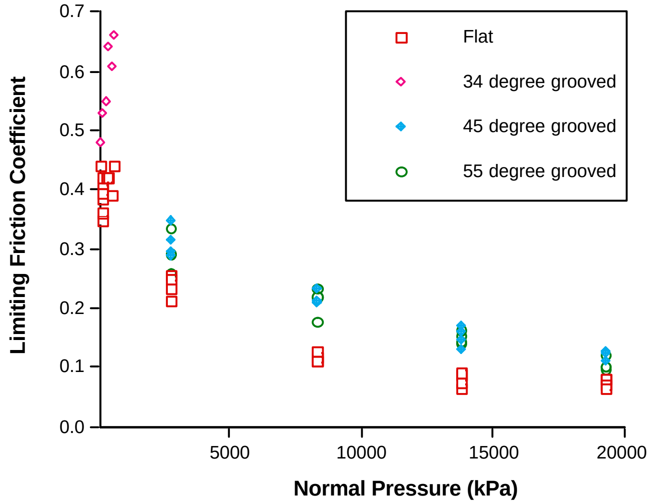

Figure 7. Limiting friction coefficient versus normal pressure for fresh prepared cane on non−rusted, machined surfaces.

reason for this convention is tentatively justified by considering the wedging action of grooves on the material (as discussed later). The smaller the included angle, the greater the wedging effect. For the case of a flat surface with no wedging effect, it follows that the included angle should represent the limit such that the included angle has been increased to its maximum value (i.e., 180°).

Normal Pressure Dependence

Figure 7 shows the limiting friction data versus normal pressure for various surface geometries. The trend of friction with normal pressure appears to decrease non−linearly, although the degree of non−linearity appears more severe for the flat surface data than for the grooved surfaces. Various non−linear forms were tested in order to identify a suitable transform for the independent variable, the result being that the logarithm of normal pressure appears linear when plotted against friction. Figure 8 shows the log plot with lines of regression for each surface geometry.

Low−pressure data are more prone to scatter than high−pressure data (which comes exclusively from Cullen's results). Bullock's low−pressure data for 34° grooving

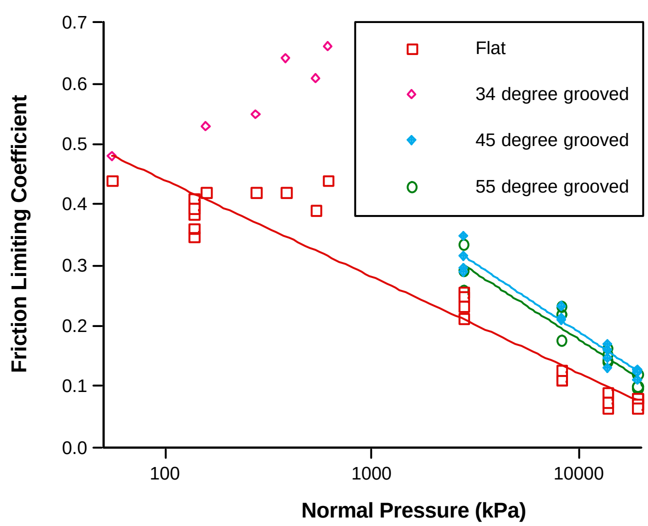

Figure 8. Log plot of figure 7 with lines of best fit for each surface geometry.

Table 4. Regression analyses for limiting friction versus normal pressure.

Surface	Log Regression	r (log reg.)	r (linear reg.)	Significance Level (log reg.)
Flat	$\mu = -0.159\log(\sigma_n) + 0.758$	0.960	0.901	<<0.1%
45° grooved	$\mu = -0.226\log(\sigma_n) + 1.096$	0.974	0.960	<<0.1%
55° grooved	$\mu = -0.219\log(\sigma_n) + 1.055$	0.958	0.960	<<0.1%

exhibits an apparently increasing trend over a relatively small range of normal pressures, which is the reverse of the expected trend. However, Bullock's original analysis of variance for this data suggested that the grooving−pressure interaction was not statistically significant. On this basis, the apparent anomaly is attributed to experimental error and not pursued. In order to confirm the validity of the log−linear regression for friction versus normal pressure, a preliminary regression analysis is given in table 4. Based on the coefficients of determination (r), the log pressure variable provides a generally better fit to the data than regression with linear pressure.

Table 4 indicates that the slope of the log−linear regression is not constant across all surface geometries. This implies that the multi−variate regression will require a second−order pressure−grooving interaction.

Limiting Shear Stress Hypothesis

A decreasing trend of friction coefficient with normal pressure is often indicative of a limiting shear stress in the weaker material. If the frictional interface is able to transmit shear stresses greater than the shear strength of the material in question, then the material will shear close to the interface, giving the impression that slip has occurred. Both Bullock and Cullen discuss the possibility of shear occurring during the friction experiments. Cullen states that slip always occurred for the flat plate, but that the grooved surface was likely to have caused shear rather than slip. The prescription of a maximum shear stress modifies the classical Coulomb friction formulation, as shown in equation 1:

$$\tau = \mu\sigma_n \left(\mu\sigma_n \le \tau_{crit}\right)$$
$$\tau = \tau_{crit} \left(\mu\sigma_n > \tau_{crit}\right)$$
$$\mu^* = \min\left(\mu, \frac{\tau_{crit}}{\sigma_n}\right) \tag{1}$$

where

τ = shear stress across the interface
σ_n = normal pressure across the interface
μ = coefficient of friction under normal conditions
μ^* = effective friction coefficient when $\tau = \tau_{crit}$
τ_{crit} = limiting (critical) shear stress.

Figure 9 shows a comparison between a predicted friction−pressure relation using the limiting shear stress formulation ($\mu = 0.4$; $\tau_{crit} = 1000$ kPa) and the experimental results for limiting friction on flat surfaces. The limiting shear stress model predicts a non−linear decrease in the friction coefficient with normal pressure in a qualitatively similar manner to the experimentally observed data. This may support the hypothesis that frictional sliding at higher pressures is actually due to local shearing of the fibrous solid

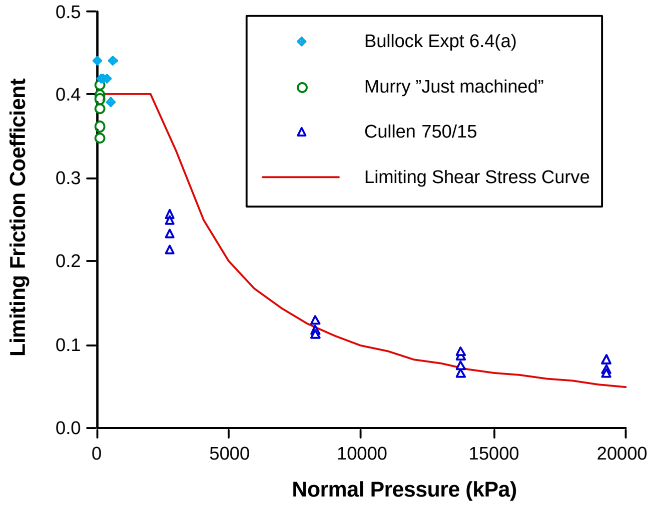

Figure 9. Limiting shear stress model compared to zero−speed frictional data for flat machined iron and steel surfaces.

matrix (at least for grooved surfaces). Alternatively, it may suggest that the observed behavior is due to some other shear stress limiting mechanism, since the assumption of constant shear strength is rather simplistic for a fibrous solid matrix that undergoes significant plastic deformation. The large degree of plastic strain hardening that occurs during compression of the sugarcane blanket would suggest that τ_{crit} will increase in some manner along with σ_n, thus invalidating the limiting shear stress model. For this reason, the limiting shear stress model is not pursued further.

Rubbing Speed Dependence

Figure 10 shows the coefficient of friction versus rubbing speed for various surface geometries and both low and high normal pressures. Regression lines are shown for each data set. Data for normal pressures less than 650 kPa are grouped together to simplify presentation, on the basis that the friction−normal pressure interaction does not have a significant effect in the low normal pressure range. The friction coefficient appears to decrease linearly with rubbing speed for all cases shown. An analysis of the regression equations

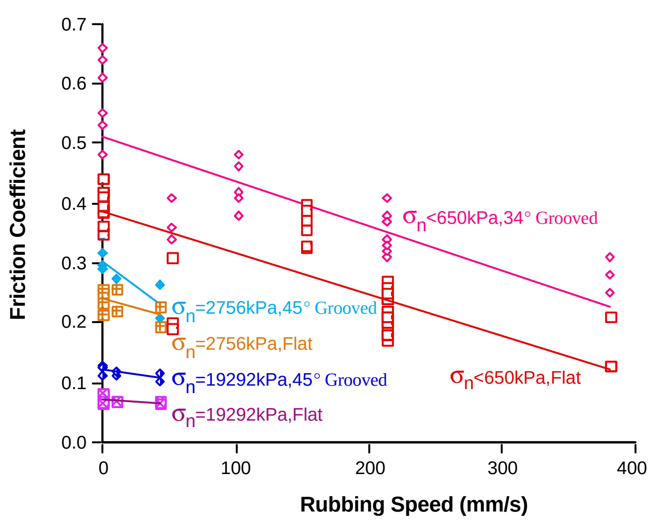

Figure 10. Coefficient of friction versus rubbing speed for flat and grooved surfaces at low and high normal pressures.

Table 5. Regression analyses for friction versus rubbing speed.

Data Set	Linear Regression	r	Significance Level
s_n < 650 kPa			
flat surface	$\mu = -6.92e-4(S_r) + 0.385$	0.803	<<0.1%
34° grooved	$\mu = -7.44e-4(S_r) + 0.511$	0.768	<<0.1%
s_n = 2756 kPa			
flat surface	$\mu = -6.45e-4(S_r) + 0.240$	0.559	7.9%
45° grooved	$\mu = -1.71e-3(S_r) + 0.303$	0.763	1.3%
s_n = 19292 kPa			
flat surface	$\mu = -1.87e-4(S_r) + 0.074$	0.500	10.9%
45° grooved	$\mu = -2.95e-4(S_r) + 0.121$	0.604	5.9%

to quantify the linear regression significance is given in table 5.

Only the flat surface data at a normal pressure of 19292 kPa are not significant at the 10% level. A further regression analysis using a second−order polynomial fit to the data sets showed marginal improvement in the significance levels, yielding a maximum significance level of 9%. However, the improvement is not enough to warrant inclusion of a second−order rubbing speed term in the main regression analysis. Note that a substantial proportion of the scatter about the rubbing speed regression lines is due to repeat data points. For example, the flat surface data at a normal pressure of 19292 kPa contains four data points at zero speed (limiting friction), two at 9 mm s^{-1}, and two at 42 mm s^{-1}. The friction coefficients at zero speed range from 0.065 to 0.082, a variation of 26%. If the repeat points were averaged before regression, the linear trend with speed would exhibit a higher coefficient of determination, although the number of data points for each high−pressure data set would be reduced to only three.

Groove Angle Dependence

Figure 11 shows the dependence of the friction coefficient on included grooving angle with lines of best fit for each data set. There is obviously a lack of experimental data for this interaction, and the available data exhibit considerable scatter in the repeat data points. Nevertheless, there is a definite tendency for the friction coefficient to decrease with

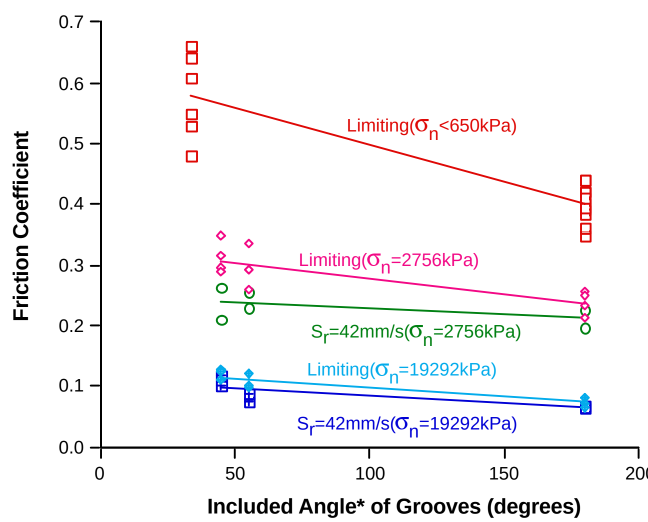

*Flat Platens are considered equivalent to 180° grooving

Figure 11. Coefficient of friction versus grooving angle for various rubbing speeds with low and high normal pressures.

Table 6. Regression analyses for friction versus groove included angle.

Data Set	Linear Regression	r	Significance Level
Limiting			
σ_n < 650 kPa	$\mu = -1.20e-3(G_\alpha) + 0.619$	0.888	<<0.1%
σ_n = 2756 kPa	$\mu = -5.02e-4(G_\alpha) + 0.328$	0.804	<0.1%
σ_n = 19292 kPa	$\mu = -3.03e-4(G_\alpha) + 0.129$	0.885	<<0.1%
S_r = 42 mm s^{-1}			
σ_n < 650 kPa	$\mu = -2.04e-4(G_\alpha) + 0.249$	0.533	15.2%
σ_n = 19292 kPa	$\mu = -2.36e-4(G_\alpha) + 0.108$	0.778	3.6%
	Power Regression		
Limiting			
σ_n < 650 kPa	$\mu = 1.227(G_\alpha)^{-0.215}$	0.891	<<0.1%
σ_n = 2756 kPa	$\mu = 0.628(G_\alpha)^{-0.187}$	0.828	<<0.1%
σ_n = 19292 kPa	$\mu = 0.411(G_\alpha)^{-0.329}$	0.913	<<0.1%
S_r = 42 mm s^{-1}			
σ_n < 650 kPa	$\mu = 0.335(G_\alpha)^{-0.088}$	0.523	15.6%
σ_n = 19292 kPa	$\mu = 0.301(G_\alpha)^{-0.295}$	0.849	1.5%

increasing grooving angle. This trend clarifies the previous assumption of flat surfaces being equivalent to 180° grooving, since the downward trend of the friction coefficient with increasing angle is preserved. The physical basis for this trend is most likely connected with the wedging effect of the grooves and is examined theoretically in the next section.

Bearing in mind the sparsity of data points, both linear and non−linear regression analyses were performed for the data sets of figure 11, with results given in table 6. Only one data set is not significant at the 10% level for both regression types. The power−law regression provides the best regression of the non−linear forms that were tested, and exhibits slightly higher coefficients of determination than linear regression. However, the small increase in the coefficients of determination does not warrant addition of a non−linear form of grooving variable into the multi−variate regression. In addition to this, the grooving angle exponent for the non−linear regression varies between about −0.1 and −0.3, and at best only an average value could be prescribed. For these reasons, a linear form of the grooving angle variable (G_α) will be used in the multi−variate regression.

Table 7. Variables used in multi−variate regression analyses for friction coefficient.

Regression	Variables	Form of Variables
Overall	s_n, S_r, G_a	$\log_e(\sigma_n)$, S_r, G_α
Flat surface	s_n, S_r	$\log_e(\sigma_n)$, S_r
55° grooved surface	s_n, S_r	$\log_e(\sigma_n)$, S_r

Multi−Variate Regression

Having considered the form of friction response against each of the three experimental variables, conclusions may be drawn regarding the most appropriate form of the variables for an overall multi−variate regression. Due to the lack of conclusive experimental data over a wide range of grooving angles, the regression must be used with caution in terms of its ability to predict grooving angle effects. For this reason, two additional multi−variate regressions are performed, each using data for only one surface geometry (i.e., the flat and 55° grooved surfaces). Each of these regressions has only two independent variables, and simplifies the friction model for the case of flat or 55° grooved surfaces. Table 7 gives details of the variables to be used in each multi−variate regression and the particular form of the factor adopted in each case.

The analysis of variance for overall multi−variate regression is shown in table 8. Results for a linear form of normal pressure variable are shown first, and comparison with the non−linear form shows the improved fit to the data obtained

Table 8. Overall multi−variate regression analysis for friction coefficient.

Model	Factors in Model	Coefficient	Standard Error	t−Value	Significance Level	Coefficient of Determination (r)
Linear	Intercept	4.26e−1	1.86e−2	22.94	<<0.1%	0.84
(1st, 2nd, and 3rd	s_n	−1.68e−5	1.80e−6	−9.37	<<0.1%	(α << 0.1%)
order interactions)	S_r	−2.73e−4	1.22e−4	−2.24	<2.5%	
	G_α	−5.11e−4	1.44e−4	−3.54	<0.1%	
	$S_r G_\alpha$	−1.03e−6	9.00e−7	−1.14	<25%	
	$s_n G_a$	2.66e−9	1.51e−8	0.18	−−	
	$s_n S_r$	−1.51e−8	5.93e−8	−0.25	−−	
	$s_n S_r G_a$	9.41e−11	5.25e−10	0.18	−−	
Non−linear	Intercept	10.30e−1	4.88e−2	21.19	<<0.1%	0.91
(1st, 2nd, and 3rd	$\log_e(\sigma_n)$	−9.05e−2	5.81e−3	−15.60	<<0.1%	(α << 0.1%)
order interactions)	S_r	−2.81e−3	5.40e−4	−5.20	<0.1%	
	G_α	−1.55e−3	3.56e−4	−4.34	<0.1%	
	$S_r G_\alpha$	4.76e−6	3.82e−6	1.25	<25%	
	$\log_e(\sigma_n) G_\alpha$	1.15e−4	4.37e−5	2.62	<0.5%	
	$\log_e(\sigma_n) S_r$	3.69e−4	8.98e−5	4.12	<0.1%	
	$\log_e(\sigma_n) S_r G_\alpha$	−7.69e−7	6.49e−7	−1.19	<25%	
Non−linear	Intercept	10.0e−1	3.68e−2	27.20	<<0.1%	0.91
(1st and 2 × 2nd	$\log_e(\sigma_n)$	−8.65e−2	4.51e−3	−19.19	<<0.1%	(α << 0.1%)
order interactions)	S_r	−2.21e−3	2.60e−4	−8.50	<<0.1%	
	G_α	−1.27e−3	2.38e−4	−5.32	<0.1%	
	$\log_e(\sigma_n) G_\alpha$	8.01e−5	3.15e−5	2.54	<1.0%	
	$\log_e(\sigma_n) S_r$	2.74e−4	4.44e−5	6.17	<0.1%	
Non−linear	Intercept	8.69e−1	2.78e−2	31.20	<<0.1%	0.88
(1st order	$\log_e(\sigma_n)$	−6.84e−2	2.99e−3	−22.83	<<0.1%	(α << 0.1%)
terms only)	S_r	−6.40e−4	5.90e−5	−10.85	<<0.1%	
	G_α	−7.24e−4	7.14e−5	−10.14	<<0.1%	

with a log form of the normal pressure, although the linear regression itself is significant at the 0.1% level. The non−linear regression using all interaction terms suggested that the third−order interaction and one of the second−order interactions was not very significant, and these terms were removed without reducing the coefficient of determination or level of significance. Finally, a non−linear regression using only first−order terms is shown for comparison. This model is also significant at the 0.1% level, but the coefficient of determination is slightly lower than the model with two second−order interactions.

Equation 2 gives the resulting overall regression equation for the friction coefficient between fresh prepared cane and non−rusted, machined, iron, or steel surfaces:

$$\mu = 1.00 - 8.65\times10^{-2}\log_e(\sigma_n) - 2.21\times10^{-3}S_r - 1.27\times10^{-3}G_\alpha + 8.01\times10^{-5}\log_e(\sigma_n)G_\alpha + 2.74\times10^{-4}\log_e(\sigma_n)S_r \qquad (2)$$

where

μ = friction coefficient

σ_n = normal pressure across the interface (kPa)

S_r = relative rubbing speed between the surfaces (mm s^{-1})

G_α = included angle of the grooving (degrees; G_α = 180° for flat surfaces).

Equations 3 and 4 give the surface−specific regressions for flat and 55° grooved surfaces, respectively. For equation 3, a second−order term is included since although regression using only first−order terms is significant at the 0.1% level, the second−order term improves the coefficient of determination. The regression of equation 4 is also significant at the 0.1% level, and in this case addition of second−order terms does not improve the coefficient of determination:

$$\mu = 7.55\times10^{-1} - 6.97\times10^{-2}\log_e(\sigma_n) - 2.00\times10^{-3}S_r + 2.40\times10^{-4}\log_e(\sigma_n)S_r \qquad (3)$$

$$\mu = 10.2\times10^{-1} - 9.05\times10^{-2}\log_e(\sigma_n) - 8.06\times10^{-4}S_r \qquad (4)$$

Discussion

Bullock's maximum experimental rubbing speed of 380 mm s^{-1} is much higher than is likely to occur in existing mills. Even if the relative rubbing speed at entry or exit to the rolls reached 50% of the roll surface speed, this would correspond to maximum rubbing speeds of approximately 120 to 130 mm s^{-1}. Over this range, the flat surface regression equation decreases monotonically for increasing normal pressure.

The observed decrease in the friction coefficient with increased rubbing speed suggests an interaction between the drainage ability of a surface and its frictional behavior. Light pressure is sufficient to cause juice expression from prepared sugarcane, so all of the frictional measurements in this analysis represent "lubricated" surface conditions. However, very high juice outflow rates through partially blocked grooves may be enough to cause build−up of juice pressures and an apparent reduction in friction coefficient due to reduced normal pressure between the fibrous blanket and the roll surface.

The log pressure terms in all three regression equations create a sharp increase in the friction coefficient for very low normal pressures. While this does not cause any difficulty over the range of experimental data, the regressions will predict physically unreasonable friction coefficients if extrapolated back to very small normal pressures. Numerical simulations of the rolling process using these regression equations will always have some zone of very small normal pressure, and it may be necessary to cap the friction coefficient for normal pressures less than the smallest experimental value (34 kPa).

In order to compare the overall regression equation with flat and grooved surface regressions, the ratio of predictions for overall versus flat and overall versus grooved regressions was determined. In each case, the appropriate grooving angle was substituted into the overall regression equation. Predicted friction coefficients differ by up to 40% for extremities of normal pressure and rubbing speed. In the range of the experimental data, however, agreement is generally better than 10%. This confirms the ability of the overall regression equation to reproduce experimentally observed friction−grooving behavior, and suggests that the overall regression equation may be used cautiously with other grooving angles.

The foregoing analysis indicates that the three regression equations provide a good fit to the experimental data for fresh prepared cane on machined iron or steel surfaces. The effects of grooving have been quantified in terms of the included angle of the grooves, although the effects of roll arcing on the friction coefficient have not been quantified. The friction regressions provide a useful tool for incorporation into numerical simulations of the crushing process.

Analysis of the Increased Frictional Grip of Grooved Surfaces

The actual mechanism by which grooved surfaces increase the friction coefficient has not been investigated by any of the previously mentioned researchers. We hypothesize that wedging of the fibrous solid matrix between the flanks of the grooves is an important factor in increasing the frictional grip of grooved surfaces, as demonstrated by the following simple wedge analysis.

Consider the partially filled roll groove shown in figure 12. Symmetry allows consideration of only half of the groove, and the area of contact of cane on the groove is idealized as an inclined plane at angle $G_\alpha/2$ to the y axis. An evenly distributed vertical compressive stress applied to the material has resultant force F_y. This force induces a normal force N across the interface, frictional force μN tangential to the interface (where μ is the local friction coefficient), and horizontal force F_x to balance the sideways thrust caused by the inclined groove flank.

For equilibrium, the forces F_x and F_y must be balanced by the resultant normal and tangential forces across the interface (N and μN). No shear forces exist along the vertical boundaries due to the symmetry of the problem. In reality, a shear force may exist along the horizontal element boundary. However, as a first approximation, this will be neglected.

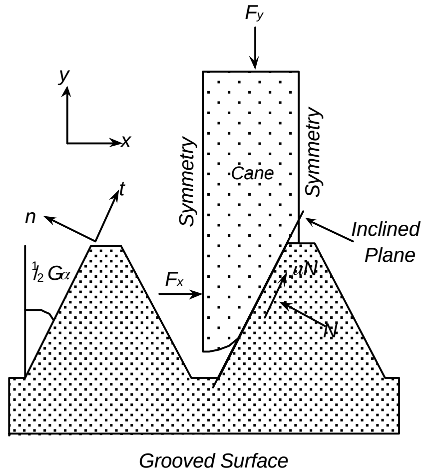

Figure 12. Forces acting on an element of material in a roll groove.

Resolving forces in the *t*−*n* coordinate system (tangential and normal to the inclined groove flank) gives:

$$F_x\cos(G_{\alpha/2}) + F_y\sin(G_{\alpha/2}) = N \qquad (5)$$

$$F_x\sin(G_{\alpha/2}) + \mu N = F_y\cos(G_{\alpha/2}) \qquad (6)$$

Substitution of equation 5 into equation 6 and rearrangement yields:

$$N = \left[\frac{\cos\left(\frac{G_\alpha}{2}\right) + \tan\left(\frac{G_\alpha}{2}\right)\sin\left(\frac{G_\alpha}{2}\right)}{\mu + \tan\left(\frac{G_\alpha}{2}\right)}\right] F_y \qquad (7)$$

For an example where the local friction coefficient $\mu = 0.2$ and groove angle $G_\alpha = 55°$, $N = 1.56F_y$.

This result indicates that a vertical force F_y acting down on the top of the element will induce a normal force of $1.56F_y$ across the interface between the groove flank and the material. Since the maximum transmissible shear force is proportional to the normal force via the local friction coefficient (neglecting any normal pressure dependence), the apparent friction coefficient has increased by the same value of 1.56, or 56%. This wedging effect clearly has potential to increase the apparent friction coefficient for grooved surfaces, and the magnitude of the increase agrees closely with experimentally measured data as shown in table 9, where the flat surface friction coefficient was taken as the true local friction coefficient in equation 7.

The flat tip region of the groove surface will tend to modify this result slightly, since the groove surface is no longer a simple inclined plane. However, this mechanism is a highly plausible explanation for the increase in apparent friction coefficient with grooved surfaces.

Table 9. Comparison of experimental and wedge analysis friction coefficients.

Surface Type	m Experimental[a]	m Wedge Analysis	Difference
Flat	0.110	0.110[b]	−−
55° grooved	0.198	0.197	0.5%
45° grooved	0.216	0.227	4.8%

[a] From Cullen (1965) at 7.7 MPa normal pressure.
[b] Experiment value.

Summary and Conclusions

A multi−variate frictional regression equation between freshly prepared sugarcane and machined surfaces was developed using the experimental data of Bullock (1957), Murry (1960), and Cullen (1965). The increased frictional grip obtained using grooved surfaces was quantified by wedge analysis of a half−groove and compared with experimentally measured values for grooved surfaces (Cullen, 1965). Several conclusions were drawn from this study:

- The friction coefficient between sugarcane and machined steel surfaces decreases with increasing normal pressure and rubbing speed, and increases for smaller included grooving angles. The friction coefficient under these conditions appears to be independent of the fineness of preparation of the material.
- The increased frictional grip of grooved surfaces is primarily caused by wedging of the material between the grooves and may be quantified using wedge analysis (the further increase in frictional grip due to roll arcing is not quantified).

Further research is required to quantify the effects of roller arcing on friction coefficient.

Acknowledgements

The authors wish to thank the Australian Sugar Research and Development Corporation for their support of this investigation.

References

Adam, C. J., and L. G. Loughran. 2001. Finite−element rolling simulation for saturated fibro−porous materials: Blanket thickness and extraction energy investigations. In *Proc. NAFEMS World Congress*, 1: 131−142. Glasgow, U.K.: NAFEMS.

Braddock, T. E. 1963. The coefficient of friction between prepared cane and metal surfaces. BE thesis. Brisbane, Australia: University of Queensland.

Bullock, K. J. 1957. An investigation into the crushing and physical properties of sugar cane and bagasse. PhD diss. Brisbane, Australia: University of Queensland.

Cullen, R. N. 1965. An investigation of the shear strength of bagasse. MEngSc thesis. Brisbane, Australia: University of Queensland.

Crawford, W. R. 1955. Mill feeding: The basic factor in efficient cane milling. *Proc. Queensland Soc. Sugar Cane Tech.* 22: 167−179.

Murry, C. R. 1960. The mechanics of crushing prepared sugar cane. PhD diss. Brisbane, Australia: University of Queensland.

Nomenclature

μ = coefficient of friction
μ^* = effective coefficient of friction when $\tau = \tau_{crit}$
σ_n = normal pressure across the interface
τ = shear stress across the interface
τ_{crit} = limiting (critical) shear stress across the interface
F_x = resultant force in the *x* direction across the cane−groove interface
F_y = resultant force in the *y* direction across the cane−groove interface
G_α = included angle of grooves
N = normal force across the cane−groove interface
r = coefficient of determination
S_r = relative rubbing speed between the surfaces